Recovery of Target Response Function for Centre-of-mass Corrections of Spherical Satellites

Toshimichi Otsubo (otsubo@crl.go.jp)
Communications Research Laboratory, 893-1 Hirai, Kashima 314-8501 Japan.
Graham M Appleby
Space Geodesy Facility, Natural Environment Research Council,
Monks Wood, Abbots Ripton, Huntingdon PE28 2LE U.K.

1. Introduction

Accurate centre-of-mass corrections for geodetic spherical satellites are expected to contribute to accurate determination of the scale of the earth, i.e., the scale of terrestrial reference frame and the geocentric gravitational constant *GM*.

Historically, a fixed centre-of-mass correction value for each satellite has been uniformly applied for all laser ranging systems. For example, a correction of 251 mm has been used for LAGEOS 1 and 2 [1], 1010 mm for AJISAI [2], and 576 mm for ETALON 1 and 2 [3]. However, the detection timing depends upon the characteristics of individual laser ranging systems and these differences cannot be ignored when we aim at the millimetre precision. Centre-of-mass corrections should, therefore, be given as system-dependent values. This is because, compared to the transmitted laser pulse, the satellite retroreflection is broadened and deformed due to reflection from multiple cube corner reflectors (so-called satellite signature effect [4]; see Fig. 1). It has nevertheless been almost impossible to precisely observe or model the actual retroreflected pulse shape. In particular, the far field diffraction effect is the most difficult to model precisely and accurately.

In this paper, we first present the basic optical retroreflection model, and then discuss how to retrieve the actual retroreflected pulse. We deal here with three types of spherical geodetic satellites, LAGEOS, AJISAI and ETALON, commonly observed by the global ILRS network.

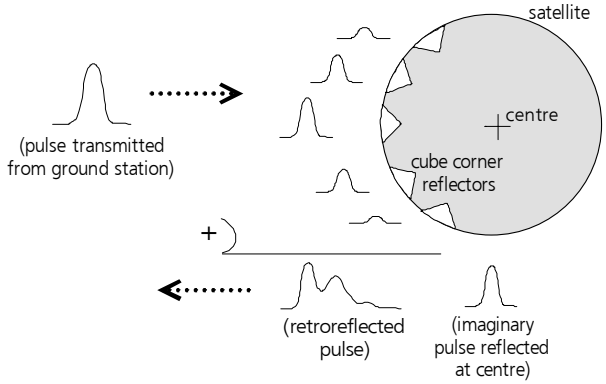

Fig. 1: Satellite signature effect.

2. Response from a single reflector

The specifications of the three types of satellites are listed in Table 1. Their diameters range from 0.60 m (LAGEOS) to 2.15 m (AJISAI). The dimensions and shapes of the reflectors also differ, as shown in Fig. 2. The aperture of the AJISAI

Table 1. Specifications of satellites.

	LAGEOS-1 / LAGEOS-2	AJISAI	ETALON-1 / ETALON-2
Launch	4 May 1976 / 22 Oct 1992	12 Aug 1986	10 Jan 1989 / 31 May 1989
Mass (kg)	411 / 405	685	1415
Approximate diameter (m)	0.60	2.15	1.294
Number of reflectors	426	1436	2146
Material of reflectors	Fused silica (422) and germanium (4)	Fused silica	Fused silica (2140) and germanium (6)

reflector is a triangle with cut vertices. That of ETALON is hexagonal, and that of LAGEOS is circular. The back faces of the ETALON reflectors are coated with aluminium, while those of the AJISAI and LAGEOS reflectors are not. The surface of each of the LAGEOS reflectors is recessed 1 mm below the surface of the reflector holder, so the front face can be partly shadowed. The holders of the AJISAI reflectors extend 2 mm above the level of the reflectors, therefore also partly obstructing the front face. Shadowing is not possible with the ETALON reflectors because the side edges of the holders are cut obliquely.

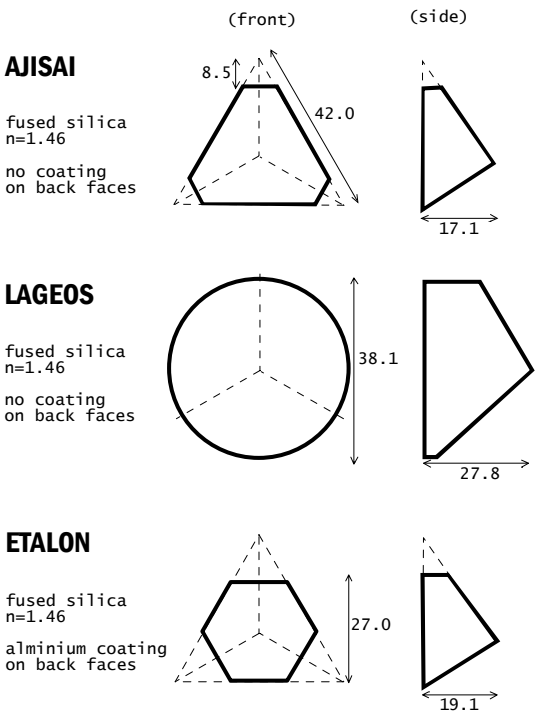

Fig. 2: Dimension of cube corner reflectors.

This variety in the reflector properties results in different effective reflection areas. The area is a function of the viewing angle and is calculated as the overlapping area of the input and output apertures [5]. We numerically calculated a 2D map of the effective reflection area for the three types of reflectors, taking into account the shadowing effect. Fig. 3 displays the results as a function of the 2D angle of incidence, where it is clear that the three types of reflectors have distinctly different characteristics.

Reflectance is modelled as a double refraction at the front face and triple reflection at the back face. It depends largely on whether the back faces of the reflectors are coated. For the uncoated reflectors of LAGEOS and AJISAI, most of the retroreflection is obtained as a result of the triple total internal reflection at the back face. As illustrated in Fig. 4, this causes a strong azimuthal reflectance pattern every 120 degrees when the angle of incidence is wider than 17

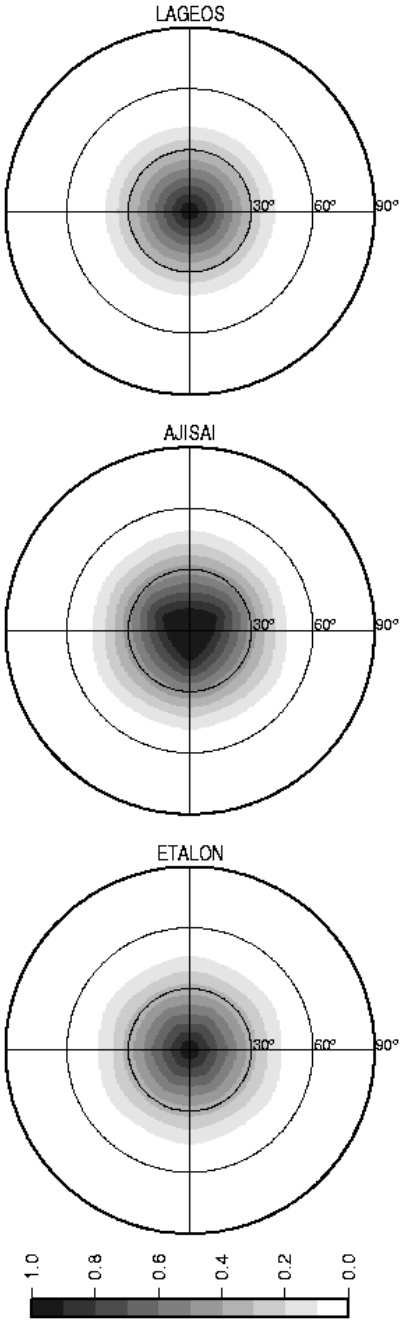

Fig. 3: Effective reflection area (normalised).

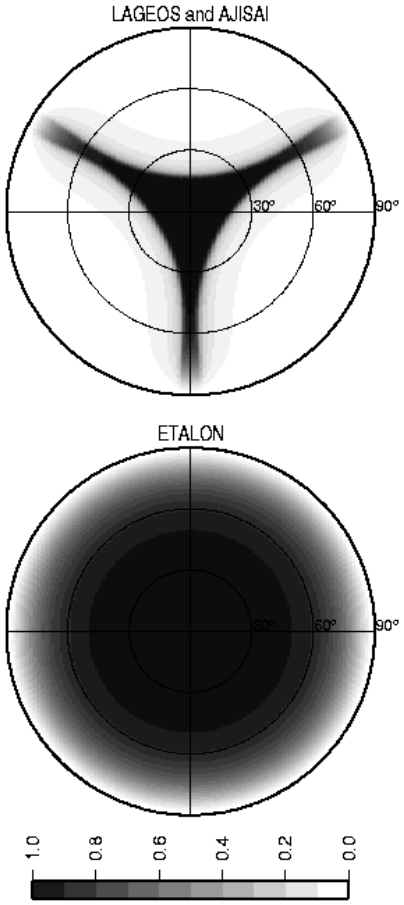

Fig. 4: Reflectance.

degrees. By contrast, the aluminium-coated ETALON reflectors have a much wider acceptance angle with no azimuthal dependence. The resulting reflectance pattern is as shown in the lower map in Fig. 4.

In this way, for an effective reflection area a and reflectance e as a function of the 2D angle of incidence, we can model the retroreflection intensity. If we neglect altogether the far-field diffraction of the reflectors, then

$$(\text{intensity}) \propto ae \quad . \qquad (1)$$

In previous studies [6-7], intensity has been modelled as

$$\text{(intensity)} \propto a^2 e \quad , \qquad (2)$$

which implicitly assumes that there is no relative motion between the satellite and terrestrial station, and that the far-field diffraction pattern is projected symmetrically around the line of sight. Neither of these two models is theoretically correct of course and we now discuss our empirical approach to solving this problem.

3. Retrieving the satellite response function

Let us now consider the response from an entire satellite. To construct a function of the retroreflection intensity for an entire satellite using knowledge of the 3D location of each of its reflectors, we have to calculate the time relations between the individual reflectors and the satellite's centre of mass [1]. We can then model the retroreflected pulse from an entire satellite by summing up the return intensities from all the reflectors, applying the delay for each. Here we neglect the effect of interference between the return signals from the different reflectors.

The remaining question is how we should model the return intensity, taking into account the diffraction effect, using models (1), (2) or something different. The approach we will adopt is to compare the models with single-photon ranging data. After computing the satellite response function as described above, we can convolve it with a function representing the response of the ranging system.

Due to velocity aberration, the far-field diffraction pattern does not fall symmetrically along the line of sight. The deviation amounts to 50 microradians (~ 10 arcseconds) at most for the geodetic satellites. The cube corner reflectors on geodetic satellites are sometimes 'spoiled' such that the angles between the reflective faces (dihedral angles) deviate slightly from 90 degrees so that the diffraction effect partly compensates for the velocity aberration. For example, the dihedral angle of the LAGEOS-2 reflectors is 90 degrees and 1.25 arcseconds with a manufacturing error of 0.5 arcseconds [1]. The AJISAI reflectors were not intentionally spoiled, but the manufacturing error amounts to 2 arcseconds. The degree or otherwise of spoiling is not known for the ETALON satellites. Thus for LAGEOS and AJISAI it would be possible to simulate the far-field diffraction pattern using the available information, but the manufacturing error prevents precise numerical computation. Moreover, we do not know the extent to which thermal deformation of a reflector disturbs the diffraction pattern. As a result, little is known about the actual diffraction effect for orbiting satellites.

Instead, we devised an empirical method for determining the profile of the response function without precisely calculating the far-field diffraction pattern. Rather than choosing either eq. (1) or (2), we chose to find the best-fit value of n in:

$$(\text{intensity}) \propto a^n e\,. \qquad (3)$$

The full-rate range residual histogram from a single photon system is useful for recovering the average response function of a satellite. Under ideal conditions with no system noise, the residual histogram of a sufficient amount of full-rate data would agree perfectly with the average response function. However, in actual data sets, the full-rate residual histogram may be considered to be a convolution of the satellite response function with the system response.

We began our search for best-fit n in eq. (3) by collecting full-rate residual histograms obtained at the NERC Herstmonceux station, United Kingdom, which adheres to a single-photon detection policy and uses a SPAD detector [4]. We used a residual histogram of the small array ERS-2 satellite ranging data to represent the system response. Since this includes an error source due to transmission of the laser pulse through the atmosphere, this is a more realistic estimate of the true system response than a residual histogram of terrestrial target ranging data. Due to the characteristics of a single-photon avalanche diode (SPAD), the residual histogram is skewed with a long tail that is cut significantly in the conventional data reduction process. However, for our use of this data to represent the system response profile, the full ERS-2 residual profile was used unedited.

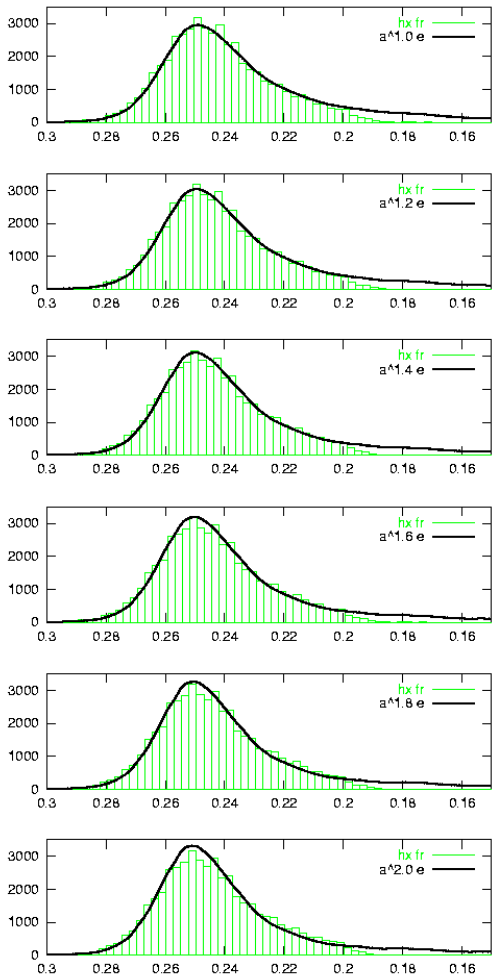

Fig. 5a: Response function vs fullrate residual histogram (LAGEOS).

The response functions of our three satellites, convolved with the ERS-2-based system response, were generated from (3) for n = 0.9 to 2.1 with a step size of 0.1. Then, the resulting distributions were compared with the Herstmonceux full-rate residual histograms for LAGEOS, AJISAI and ETALON. These residual histograms were constructed from data collected for a few tens of passes during June-July 2000 and September-October 2001 at the Herstmonceux station. We used data already filtered on site, unlike the ERS-2 data.

Six selected cases for LAGEOS, AJISAI and ETALON are shown in Fig. 5 for comparison.

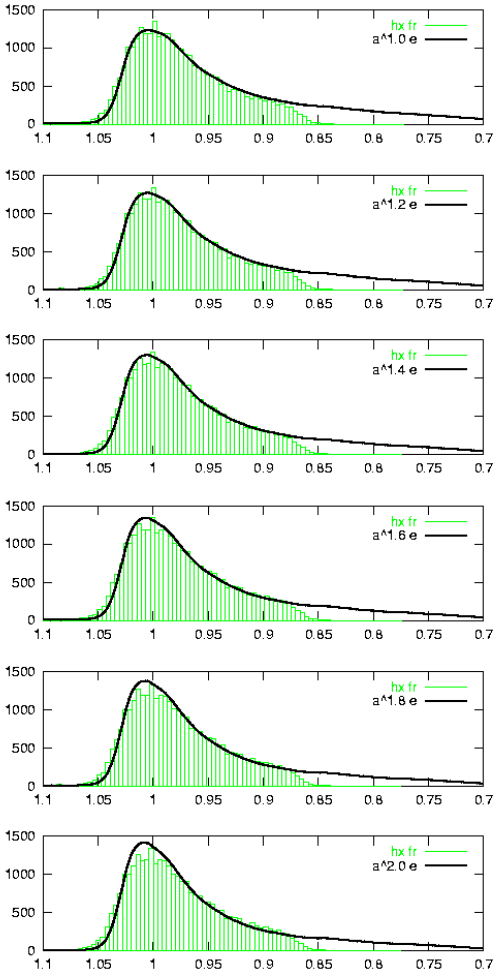

Fig. 5b: Response function vs fullrate residual histogram (AJISAI).

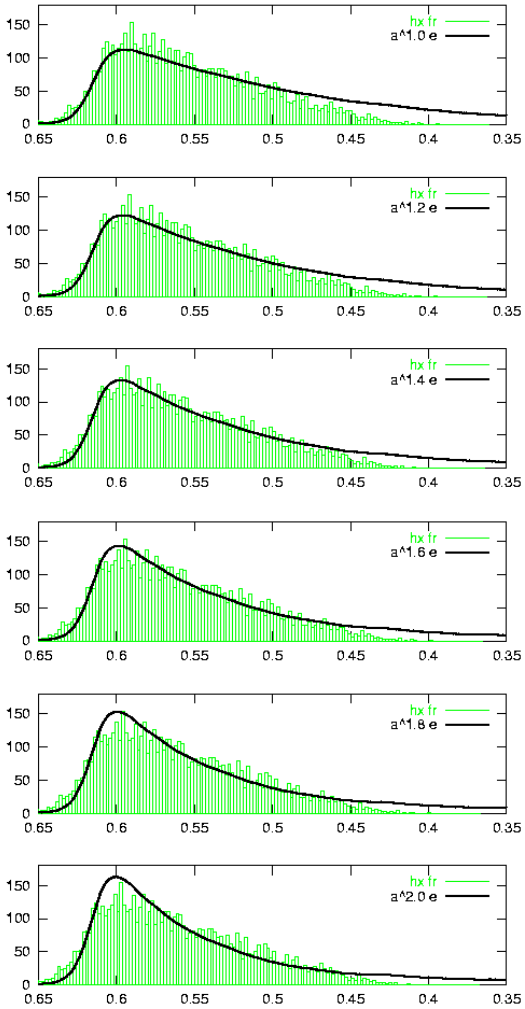

Fig. 5c: Response function vs fullrate residual histogram (ETALON).

Two parameters, the vertical scale and horizontal offset, were adjusted to fit each theoretical curve to a residual histogram. The fit with $n = 2.0$ that had been adopted in the previous studies [6-7] is clearly not very good; the response function model is too narrow. The fit is better with $n = 1.0$ in all cases.

We then used the differences between the convolved functions and the Herstmonceux residuals to estimate the best-fit n. For range data obtained during June-July 2000, the best fits were obtained for $n = 1.2$ for LAGEOS, 1.1 for AJISAI and 1.3 for ETALON. For September-October 2001 with more data, the results were 1.1 for LAGEOS (Fig. 5a), 1.2 for AJISAI (Fig. 5b), and 1.3 for ETALON (Fig. 5c).

We also obtained the full-rate data of ETALON and CHAMP (the small laser array on

CHAMP makes it another ideal target for determining system response) from the Graz laser station, Austria. The return energy in their CHAMP (low orbit) ranging was kept at a low level especially for this study, and most of the return from the high-orbiting ETALON was likely to also be at single-photon levels. Nevertheless, as Graz does not strictly keep at a single-photon level of return, we additionally rejected data whenever the return rate was higher than 10%, in order to treat only the single-photon data. Finally, applying the same procedure as for the Herstmonceux case, we obtained a best-fit n of 1.3, in good agreement with the Herstmonceux results for ETALON.

Given these consistent results, we obtained the value of parameter n:

n (LAGEOS) = 1.1
n (AJISAI) = 1.2
n (ETALON) = 1.3.

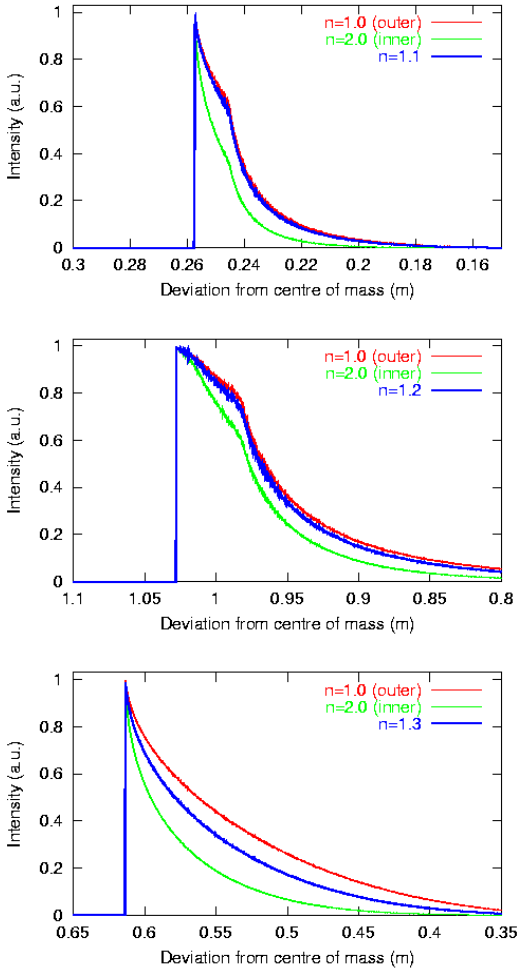

Fig. 6: Empirically derived response function for LAGEOS, AJISAI and ETALON (blue curves).

The resulting response functions for the three satellites using these values of n and convolved with negligibly narrow 1-ps FWHM Gaussian distributions to represent system noise are shown in Fig. 6. The empirically adjusted values of n for each satellite were used to compute them and also shown for comparison are the functions obtained when n was 1.0 and 2.0. When these extreme values are used, there is clearly a significant variation in the response functions. However, it is clear that the realistic uncertainty of 0.1 in our determination of n would cause only a slight change in the functions and have only marginal effect on the computed centre-of-mass corrections.

4. Conclusions

The satellite response functions for LAGEOS, AJISAI and ETALON were empirically derived using full-rate residual profiles. The results suggest that the diffraction effect must be taken into

consideration to some extent because the values of *n* were all larger than 1.0, but they also suggest that the effect is much smaller than we had assumed in previous studies because the values of *n* are significantly smaller than 2.0.

System dependent centre-of-mass corrections for these satellites were also calculated [8] based on these empirically derived response functions. The corrections vary about by 1 cm for LAGEOS and by 4-5 cm for AJISAI and ETALON.

Acknowledgment

We thank Dr. Roger Wood, NERC Space Geodesy Facility, U.K., and Dr. Georg Kirchner, Austrian Academy of Sciences, for the full-rate laser ranging data from Herstmonceux and Graz respectively.

References

[1] P. O. Minott, T. W. Zagwodzki, T. Varghese and M. Selden, "Prelaunch optical characterization of the Laser Geodynamic Satellite (LAGEOS 2)," NASA Tech. Paper, TP-3400, 1993.

[2] M. Sasaki and H. Hashimoto, "Launch and observation program of the experimental geodetic satellite of Japan," IEEE Trans Geosci. Remote Sens., 25, 526-533, 1987.

[3] N. T. Mironov, A. I. Emetz, A. N. Zaharov and V. E. Tchebotarev, "ETALON-1, -2 center of mass correction and array reflectivity," in Proc. 8th International Workshop on Laser Ranging Instrumentation, 6.9-6.32, 1992.

[4] G. M. Appleby, "Satellite signatures in SLR observations," in Proc. 8th International Workshop on Laser Ranging Instrumentation, 2.1-2.14, 1992.

[5] D. A. Arnold, "Method of calculating retroreflector-array transfer functions," Smithsonian Astrophysical Observatory Special Rep. 382, 1979.

[6] R. Neubert, "An analytical model of satellite signature effects," Proc. 9th International Workshop on Laser Ranging Instrumentation, 82-91, 1994 (some minor corrections available at http://www.gfz-potsdam.de/pb1/SLR/tiger/signat.htm).

[7] T. Otsubo, J. Amagai and H. Kunimori, "The center-of-mass correction of the geodetic satellite AJISAI for single-photon laser ranging," IEEE Trans Geosci. Remote Sens., 37, 4, 2011-2018, 1999.

[8] T. Otsubo and G. M. Appleby, "System-dependent centre-of-mass correction for spherical geodetic satellites," submitted to J. Geophy. Res., 2002.